



Mie Scattering and Characteristic Modes of Lossy Dielectric Objects

Henrik Wallén*, Pasi Ylä-Oijala, Dimitrios C. Tzarouchis, and Ari Sihvola
Department of Electronics and Nanoengineering, Aalto University, Finland

Abstract

Using Mie scattering, we derive the characteristic modes of both conducting and dielectric spheres. The results also provide a physically clear interpretation of the imaginary part of the characteristic eigenvalues for lossy objects in general.

1 Introduction

The theory of characteristic modes (TCM) provides orthogonal sets of eigenmodes for radiated and scattered fields for objects of arbitrary shape. TCM has recently become a popular tool in the antenna community, as the characteristic eigencurrents provide excitation independent insight into the antenna design process. The general theory was originally proposed by Garbacz [1, 2] and most implementations and applications are today based on the Harrington–Mautz formulation for perfectly conducting (PEC) objects [3].

For dielectric objects, TCM has been far less popular due to the lack of a surface integral equation (SIE) based formulation with the same properties as in the PEC case. In a companion presentation [4], we propose a new SIE-based TCM-formulation and describe why it is free from the spurious modes that have plagued previous SIE-TCM formulations.

In this presentation, we revisit the pioneering work by Garbacz [1, 2] and its connection to Mie series. In particular, we get analytical expressions for the TCM eigenvalues (and fields) for both PEC and dielectric spheres. In addition, the new TCM results for lossy spheres also lead to a very clear interpretation of the imaginary part of a TCM eigenvalue: it is simply the ratio of dissipated and radiated power.

2 Mie Scattering

Following Bohren and Huffman [5], with the time convention $e^{-i\omega t}$, the incident electric field is the linearly polarized plane wave

$$\mathbf{E}^i = E_0 e^{ikr \cos \theta} \hat{\mathbf{e}}_x = \sum_{n=1}^{\infty} E_n \left(\mathbf{M}_{o1n}^{(1)} - i \mathbf{N}_{e1n}^{(1)} \right), \quad (1)$$

where $E_n = i^n E_0 (2n+1)/[n(n+1)]$ and explicit expressions for the vector multipoles \mathbf{M}, \mathbf{N} and explanation of their indices can be found in [5, Sec. 4.3.1]. The scattered electric field is

$$\mathbf{E}^s = \sum_{n=1}^{\infty} E_n \left(ia_n \mathbf{N}_{e1n}^{(3)} - b_n \mathbf{M}_{o1n}^{(3)} \right), \quad (2)$$

where the Mie-scattering coefficients a_n (TM) and b_n (TE) for a dielectric sphere with (possibly complex) relative permittivity ε_r and radius a are

$$a_n = \frac{m \psi_n(mx) \psi_n'(x) - \psi_n(x) \psi_n'(mx)}{m \psi_n(mx) \xi_n'(x) - \xi_n(x) \psi_n'(mx)}, \quad (3)$$

$$b_n = \frac{\psi_n(mx) \psi_n'(x) - m \psi_n(x) \psi_n'(mx)}{\psi_n(mx) \xi_n'(x) - m \xi_n(x) \psi_n'(mx)}, \quad (4)$$

where $m = \sqrt{\varepsilon_r}$, $\mu_r = 1$, $x = ka$ and the Riccati–Bessel functions ψ_n, ξ_n are

$$\psi_n(\rho) = \rho j_n(\rho), \quad \xi_n(\rho) = \rho h_n^{(1)}(\rho), \quad (5)$$

where j_n and $h_n^{(1)}$ are the usual spherical Bessel and Hankel functions. For a PEC sphere, the coefficients simplify to

$$a_n^{\text{PEC}} = \frac{\psi_n'(x)}{\xi_n'(x)}, \quad b_n^{\text{PEC}} = \frac{\psi_n(x)}{\xi_n(x)}, \quad (6)$$

while expressions for the scattering coefficients for spheres with arbitrary (possibly complex) ε_r and μ_r can be found in [5, Sec. 4.3.3].

From (1) and (2) we can separate the TE and TM components of the total field $\mathbf{E} = \mathbf{E}^i + \mathbf{E}^s$ for each degree n as

$$\mathbf{E}_n^{\text{TE}} = E_n \left[\mathbf{M}_{o1n}^{(1)} - b_n \mathbf{M}_{o1n}^{(3)} \right], \quad (7)$$

$$\mathbf{E}_n^{\text{TM}} = -i E_n \left[\mathbf{N}_{e1n}^{(1)} - a_n \mathbf{N}_{e1n}^{(3)} \right]. \quad (8)$$

Using the above formulas, we can calculate the electric field anywhere outside the sphere, but it is often convenient to express the overall response using the extinction, scattering, and absorption efficiencies [5]

$$Q_{\text{ext}} = \frac{2}{x^2} \sum_{n=1}^{\infty} (2n+1) \text{Re}\{a_n + b_n\}, \quad (9)$$

$$Q_{\text{sca}} = \frac{2}{x^2} \sum_{n=1}^{\infty} (2n+1) \left(|a_n|^2 + |b_n|^2 \right), \quad (10)$$

$$Q_{\text{abs}} = Q_{\text{ext}} - Q_{\text{sca}}. \quad (11)$$

3 Characteristic Modes of a Sphere

In Garbacz' original work [1, 2] the characteristic equation is

$$\alpha_n \mathbf{F}_n(\theta, \phi) = \mathcal{P} \mathbf{F}_n(\theta, \phi), \quad (12)$$

where α_n is the complex characteristic value for the perturbation operator \mathcal{P} and \mathbf{F}_n is the corresponding characteristic far-field pattern function of an incoming or outgoing spherical wave. The complex characteristic value can, moreover, be expressed as

$$\alpha_n = \frac{-1}{1 - i \lambda_n} \quad \Leftrightarrow \quad \lambda_n = \frac{1 + \alpha_n}{i \alpha_n}, \quad (13)$$

where λ_n is real if the scatterer is lossless and λ_n is identical to the TCM eigenvalue in the surface integral formulations following [3]. (Notice, however, differences in time-conventions.)

The perturbation operator is defined in the following way: We start with an incoming field f^i , which is essentially a vector multipole with $h_n^{(2)}(kr)$. The corresponding outgoing field f^o has similarly $h_n^{(1)}(kr)$. In the absence of any scatterer $f^o = \mathcal{I} f^i$, with a suitably defined identity operator \mathcal{I} . Garbacz defines the scattered field $f^s = \mathcal{P} f^i$ as one half of the perturbation of the outgoing field due to the scatterer, that is, the total field is

$$f^i + f^o + 2f^s = f^i + f^o + 2\mathcal{P} f^i = f^i + f^o + 2\alpha_n f^o. \quad (14)$$

In the TE_{mn} case, we can express the total electric field using the Bohren–Huffman vector multipoles in the form

$$\begin{aligned} \mathbf{E}^{\text{TE}} &= \underbrace{E_0^{\text{TE}} \mathbf{M}_{xmn}^{(4)}}_{f^i} + \underbrace{E_0^{\text{TE}} \mathbf{M}_{xmn}^{(3)}}_{f^o} + 2\alpha_n^{\text{TE}} E_0^{\text{TE}} \mathbf{M}_{xmn}^{(3)} \\ &= 2E_0^{\text{TE}} \left[\mathbf{M}_{xmn}^{(1)} + \alpha_n^{\text{TE}} \mathbf{M}_{xmn}^{(3)} \right], \end{aligned} \quad (15)$$

where E_0^{TE} is a complex constant depending on the normalization of the fields, the subscript x can be either e (even) or o (odd), and the relation $\mathbf{M}_{xmn}^{(4)} + \mathbf{M}_{xmn}^{(3)} = 2\mathbf{M}_{xmn}^{(1)}$ follows straightforwardly from the properties of the spherical Hankel and Bessel functions $h_n^{(2)} + h_n^{(1)} = 2j_n$. In the TM_{mn} case, we similarly get

$$\begin{aligned} \mathbf{E}^{\text{TM}} &= E_0^{\text{TM}} \mathbf{N}_{xmn}^{(4)} + E_0^{\text{TM}} \mathbf{N}_{xmn}^{(3)} + 2\alpha_n^{\text{TM}} E_0^{\text{TM}} \mathbf{N}_{xmn}^{(3)} \\ &= 2E_0^{\text{TM}} \left[\mathbf{N}_{xmn}^{(1)} + \alpha_n^{\text{TM}} \mathbf{N}_{xmn}^{(3)} \right]. \end{aligned} \quad (16)$$

Comparing the relative amplitude of the scattered and incident electric fields in (15) vs (7) and (16) vs (8), we get

$$\alpha_n^{\text{TE}} = -b_n, \quad \alpha_n^{\text{TM}} = -a_n. \quad (17)$$

Therefore, the TCM eigenvalues for a sphere can be written in terms of the Mie-scattering coefficients as

$$\lambda_n^{\text{TE}} = \frac{b_n - 1}{i b_n}, \quad \lambda_n^{\text{TM}} = \frac{a_n - 1}{i a_n}. \quad (18)$$

In both the TE and TM cases, the indices xm do not affect the radial functions and so the complex characteristic values only depend on the polarization (TE/TM) and degree n . The modes are degenerated, so that each eigenvalue λ_n has multiplicity $2n + 1$.

The result (18) works for both PEC and material spheres, as long as the appropriate Mie-scattering coefficients are used. The result agrees with [6] in the PEC case.

4 Interpretation of the TCM Eigenvalues

For both PEC and lossless dielectric spheres, the TCM eigenvalues λ_n are real, as they should be for any lossless scatterer of arbitrary shape [1, 2]. The eigenvalue for a lossless scatterer or the real part of the eigenvalue of a lossy scatterer should, in general, be related to stored energy in the same way as for PEC scatterers [3].

The interpretation of the imaginary part of the TCM eigenvalue is, however, much less known. In [7] Harrington, Mautz and Chang developed two alternative volume integral equation based TCM formulations for lossy dielectric bodies. Depending on the choice of the formulation, the obtained eigenvalues were either complex or real. However, any comprehensive study of the role of the imaginary part of the eigenvalue was not provided. SIE-based formulations for dielectric objects following [8] produce spurious results, as discussed in [9], and it appears that the imaginary part of the eigenvalues has not been given any attention.

For a single characteristic mode and its corresponding Mie-scattering coefficient $c_n = a_n, b_n$, we have

$$\lambda_n = \frac{c_n - 1}{i c_n}, \quad c_n = \frac{1}{1 - i \lambda_n}, \quad (19)$$

and the scattering and absorption efficiencies (10) and (11) simplify to

$$Q_{\text{sca}} = \frac{2}{x^2} (2n + 1) |c_n|^2, \quad (20)$$

$$Q_{\text{abs}} = \frac{2}{x^2} (2n + 1) \left[\text{Re}\{c_n\} - |c_n|^2 \right]. \quad (21)$$

It is fairly straightforward to show that for any complex c_n , we get

$$\text{Im}\{\lambda_n\} = \frac{\text{Re}\{c_n\} - |c_n|^2}{|c_n|^2} = \frac{Q_{\text{abs}}}{Q_{\text{sca}}} = \frac{P_{\text{abs}}}{P_{\text{sca}}} \geq 0. \quad (22)$$

Therefore, the imaginary part of the TCM eigenvalue is simply the ratio of absorbed and scattered power, or equivalently from an antenna perspective, the ratio of dissipated and radiated power.

For the real part of the eigenvalue, we similarly get

$$\text{Re}\{\lambda_n\} = \frac{\text{Im}\{c_n\}}{|c_n|^2}, \quad (23)$$

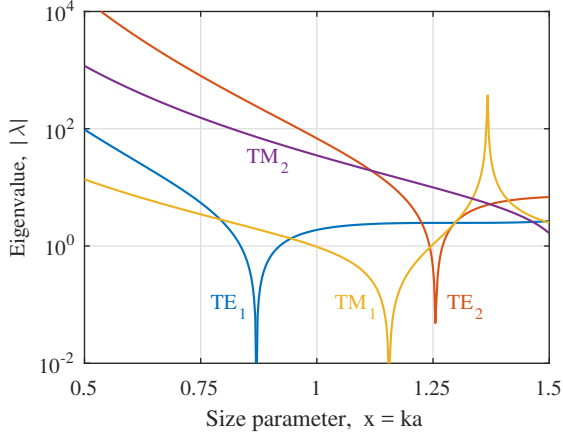


Figure 1. Magnitude of the TCM eigenvalues for a dielectric sphere with $\epsilon_r = 12$. Only the first two TE and TM eigenvalues are shown.

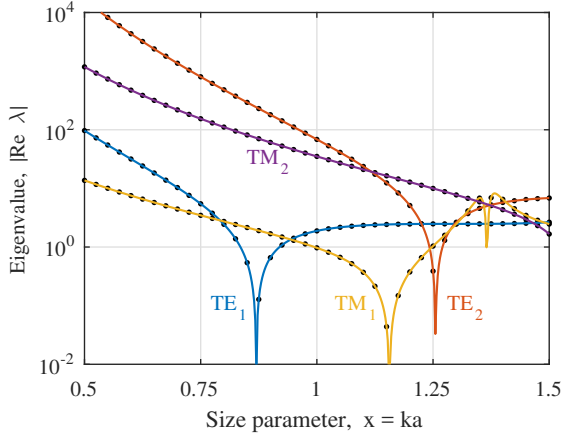


Figure 2. Magnitude of the real part of the TCM eigenvalues for a lossy dielectric sphere with $\epsilon_r = 12 + 0.24i$. The SIE results are plotted using black dots.

but it is not entirely obvious how this is related to stored energy. In the PEC case, λ_n agrees with the Harrington–Mautz solution, as is also evident from the results in [6], but it would be useful to show how (23) is related to stored energy in the general case.

A characteristic mode resonates when its eigenvalue is zero, and so the mode whose eigenvalue is smallest in magnitude dominates. Instead of looking at the magnitude of the eigenvalue, it is often convenient to study the modal significance σ_n , which has a very simple relation to the Mie coefficients

$$\sigma_n = \left| \frac{1}{1 - i\lambda_n} \right| = |c_n|, \quad (24)$$

where $c_n = a_n$ (TM) or b_n (TE).

5 Numerical Example

Figure 1 shows the first two TE and TM eigenvalues for a lossless dielectric sphere with $\epsilon_r = 12$. Three resonances

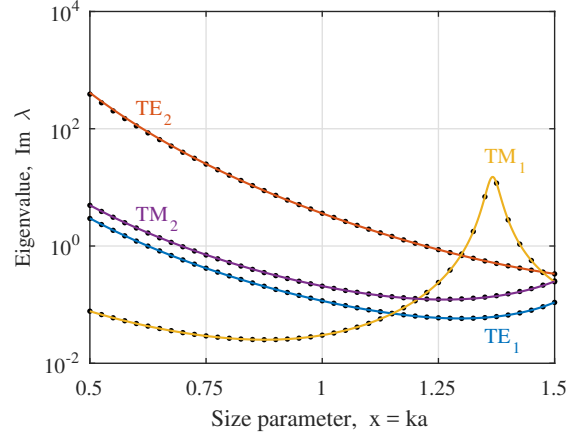


Figure 3. Imaginary part of the TCM eigenvalues for a lossy dielectric sphere with $\epsilon_r = 12 + 0.24i$. The SIE results are plotted using black dots.

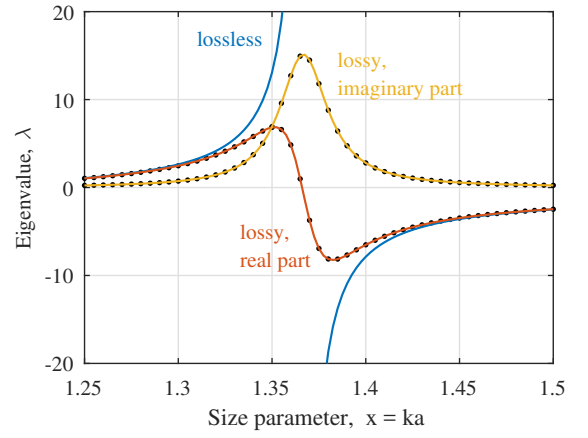


Figure 4. Comparison of the lossless and lossy TM_1 case near the absorption maximum. The SIE results are plotted using black dots.

occur in the shown size-parameter range: a magnetic dipole (TE_1) at $x = 0.87$, an electric dipole (TM_1) at $x = 1.16$, and a magnetic quadrupole (TE_2) at $x = 1.26$. The electric quadrupole resonance is slightly outside the figure at $x = 1.56$. The TM_1 peak at $x = 1.37$ corresponds to an interior resonance, which does not radiate.

Figures 2 and 3 shows the real and imaginary part of the TCM eigenvalues for the same sphere with small losses ($\epsilon_r = 12 + 0.24i$). Except for the TM_1 case near the interior resonance at $x = 1.37$, the real part of the eigenvalue is very close to the lossless case. The maximum of the imaginary part of λ_1^{TM} at $x = 1.37$ in Figure 3 shows that the internal resonance creates fairly strong absorption although the material losses are small. Otherwise, the imaginary part of the eigenvalue is relatively small compared with the real part, as one could expect when small losses are added. The behavior of the TM_1 eigenvalue looks very strange near $x = 1.37$ in Figure 2, but that is only due to the logarithmic scale. When plotted on a linear scale in Figure 4, the lossy case more clearly shows the typical features of a damped resonance.

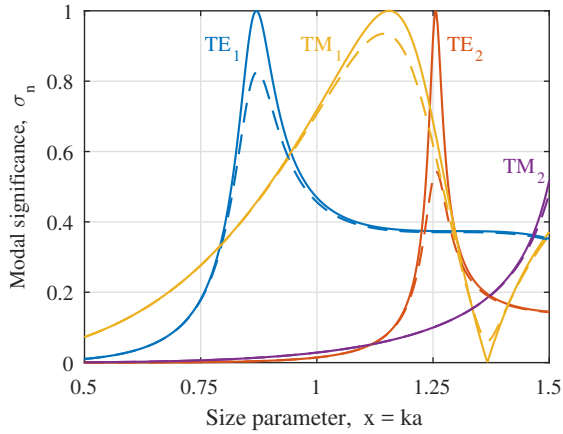


Figure 5. Modal significance of the TCM eigenvalues for a sphere with $\epsilon_r = 12$ (solid line) and $\epsilon_r = 12 + 0.24i$ (dashed line).

Figures 2–4 also include numerical results computed using the new SIE-based TCM-formulation presented in [4]. As is evident from the figures, the agreement is excellent.

Figure 5 shows the modal significance of the lowest two TE and TM eigenvalues for the same dielectric sphere in both the lossless ($\epsilon_r = 12$) and lossy ($\epsilon_r = 12 + 0.24i$) case. The same resonances as in Figures 1 and 2 can be clearly observed, but the width of the resonances and their sensitivity to losses are more clearly visible.

6 Conclusions

In this presentation, we derived analytical expressions for the characteristic eigenvalues of a sphere in terms of Mie scattering coefficients. Equivalent expressions for the PEC case can also be found in [6], but (18) is a much more general solution.

The initial motivation for deriving the analytical results was to validate a new SIE-based TCM-formulation for dielectric and magneto-dielectric objects [4]. However, the new analytical solution also provided a physically appealing interpretation of the imaginary part of a characteristic eigenvalue as the ratio between radiated and dissipated power (22).

References

- [1] R. J. Garbacz, “A generalized expansion for radiated and scattered fields,” Ph.D. dissertation, Ohio State University, 1968.
- [2] R. J. Garbacz and R. H. Turpin, “A generalized expansion for radiated and scattered fields,” *IEEE Trans. Antennas Propag.*, vol. 19, no. 3, pp. 348–358, May 1971.
- [3] R. F. Harrington and J. R. Mautz, “Theory of characteristic modes for conduction bodies,” *IEEE Trans. Antennas Propag.*, vol. 19, no. 5, pp. 622–628, Sep. 1971.
- [4] P. Ylä-Oijala, H. Wallén, D. C. Tzarouchis, and A. Sihvola, “Surface integral equation formulation for characteristic modes of lossy dielectric objects,” to be presented in *2nd URSI AT-RASC, Gran Canaria, Spain*, 28 May – 1 June 2018.
- [5] C. F. Bohren and D. R. Huffman, *Absorption and Scattering of Light by Small Particles*. John Wiley & Sons, 1983.
- [6] M. Capek, V. Losenicky, L. Jelinek, and M. Gustafsson, “Validating the characteristic modes solvers,” *IEEE Trans. Antennas Propag.*, vol. 65, no. 8, pp. 4134–4145, Aug. 2017.
- [7] R. F. Harrington, J. R. Mautz, and Y. Chang, “Characteristic modes for dielectric and magnetic bodies,” *IEEE Trans. Antennas Propag.*, vol. 20, no. 2, pp. 194–198, Mar. 1972.
- [8] Y. Chang and R. F. Harrington, “A surface formulation for characteristic modes of material bodies,” *IEEE Trans. Antennas Propag.*, vol. 25, no. 6, pp. 789–795, Nov. 1977.
- [9] Z. T. Miers and B. K. Lau, “Computational analysis and verifications of characteristic modes in real materials,” *IEEE Trans. Antennas Propag.*, vol. 64, no. 7, pp. 2595–2607, Jul. 2016.